Inorg. Chem. **2009**, *48*, 1533−1541

Two Related Gadolinium Aquo Carbonate 2-D and 3-D Structures and Their Thermal, Spectroscopic, and Paramagnetic Properties

David L. Rogow, Claudia H. Swanson, Allen G. Oliver, and Scott R. J. Oliver*

Department of Chemistry and Biochemistry, University of California, Santa Cruz, 1156 High Street, Santa Cruz, California 95064

Received September 26, 2008

We report two new extended inorganic materials based on gadolinium. The first, $[Gd(CO_3)_2H_2O][NH_4]$, consists of negatively charged 2-D sheets of gadolinium carbonate with one coordinated water molecule and an ammonium cation between the layers. The coordinated water and one carbonate extend into the interlayer space, connecting the layers via an extensive hydrogen bonding network which includes the ammonium ions. The second, a closely related yet more condensed framework structure, $[Gd_2(CO_3)_3NH_3H_2O]$, is formed at a higher hydrothermal temperature and was characterized by single crystal X-ray diffraction data collected at a synchrotron. This second structure contains layers that are isostructural to the first, bridged together by carbonate, and coordinated by water and ammonia. The properties of these materials were studied by thermogravimetric analysis−mass spectrometry, photoluminescence, electron paramagnetic resonance, and Raman and infrared spectroscopy. The 2-D $[Gd(CO_3)_2H_2O][NH_4]$ is stable to about 175 °C, though water and ammonium loss continues through the entire thermogravimetric analysis trace. The 3-D material remains intact until about 325 °C. Both structures exhibit broad luminescence bands in the near-ultraviolet region centered at 354 nm. Electron paramagnetic resonance and magnetic susceptibility show spin−spin coupling between adjacent gadolinium atoms in both structures and confirm that they are paramagnetic. These materials show interesting photoluminescent and paramagnetic properties that could possibly be exploited for chemical sensing or magnetic materials applications.

Introduction

We are interested in the design and synthesis of extended open framework inorganic solids for use as heterogeneous catalysts in addition to use as intercalation, optoelectronic, solid-state electronic, or magnetic materials. Rare earth metals have interesting luminescent and magnetic properties because of the electrons in their 4f orbitals.[1,2] New technologies being developed for rare earth containing extended solids include catalysis,[3,4] phosphors,[5,6] magnetic and magneto-optic materials,[7,8] superconductors,[9,10] and Raman lasers.[11,12] Our research group recently began investigating lanthanide metals for their range of possible geometries coupled with their potentially useful properties.[13] The original aim was to discover new solid inorganic materials where the host structures contain rare-earth metals and where uptake or exchange of a guest molecule leads to an observable change in fluorescence.

* To whom correspondence should be addressed. E-mail: soliver@chemistry.ucsc.edu.

(1) Hughes, I. D.; Dane, M.; Ernst, A.; Hergert, W.; Luders, M.; Poulter, J.; Staunton, J. B.; Svane, A.; Szotek, Z.; Temmerman, W. M. *Nature* **2007**, *446* (7136), 650–653.
(2) Bunzli, J. C. G.; Piguet, C. *Chem. Soc. Rev.* **2005**, *34* (12), 1048–1077.
(3) Voorhoev, R. J.; Remeika, J. P.; Johnson, D. W. *Science* **1973**, *180* (4081), 62–64.
(4) Mahapatra, S.; Madras, G.; Row, T. N. G. *J. Phys. Chem. C* **2007**, *111* (17), 6505–6511.
(5) Danielson, E.; Devenney, M.; Giaquinta, D. M.; Golden, J. H.; Haushalter, R. C.; McFarland, E. W.; Poojary, D. M.; Reaves, C. M.; Weinberg, W. H.; Wu, X. D. *Science* **1998**, *279* (5352), 837–839.
(6) Park, I. Y.; Kim, D.; Lee, J.; Lee, A. H.; Kim, K. J. *Mater. Chem. Phys.* **2007**, *106* (1), 149–157.
(7) Huang, M.; Xu, Z. C. *Thin Solid Films* **2004**, *450* (2), 324–328.
(8) Nan, C. W.; Li, M.; Feng, X. Q.; Yu, S. W. *Appl. Phys. Lett.* **2001**, *78* (17), 2527–2529.
(9) Chen, X. H.; Wu, T.; Wu, G.; Liu, R. H.; Chen, H.; Fang, D. F. *Nature* **2008**, *453* (7196), 761–762.
(10) Takahashi, H.; Igawa, K.; Arii, K.; Kamihara, Y.; Hirano, M.; Hosono, H. *Nature* **2008**, *453* (7193), 376–378.
(11) Piper, J. A.; Pask, H. M. *IEEE J. Sel. Top. Quantum Electron.* **2007**, *13* (3), 692–704.
(12) Dekker, P.; Pask, H. M.; Spence, D. J.; Piper, J. A. *Opt. Express* **2007**, *15* (11), 7038–7046.
(13) Rocha, J.; Carlos, L. D. *Curr. Opin. Solid State Mater. Sci.* **2003**, *7* (3), 199–205.

10.1021/ic801844b CCC: $40.75
Published on Web 01/21/2009

Doping of host solids with trivalent rare earth ions is also an area of intense research. Lanthanide metals such as Eu^{3+}, Tb^{3+}, and Er^{3+} are used as dopants in several different systems for up-conversion phosphors.[14−16] Many mixed metal compounds intrinsically contain rare earths such as $(Gd_{1-x}La_x)_2O_3$, used as a lithium ion conducting electrolyte by doping with $LiNO_3$ and KNO_3.[17] $(Gd_{1-x}La_x)_2O_3$ doped with $LiNO_3$ has also been used as an auxiliary electrode in a solid electrolyte NO gas sensor.[18] Gadolinium oxide is used as a dopant in semiconductor photocatalyst systems for the decomposition of organic pollutants and water splitting.[19] Photocatalysis is therefore another application we would like to explore with lanthanide containing solids.

Rare earth carbonate extended materials have been prepared by thermal decomposition of urea.[20] The lanthanide carbonate structures crystallize in an orthorhombic cell setting and are isostructural to the mineral tengerite, $Y_2(CO_3)_3 \cdot nH_2O$ ($n = 2-5$). There were many early reports with conflicting composition because of the poor crystallinity and polycrystallinity of these rare earth carbonates. With advances in area detectors for X-ray diffraction, the ambiguity of the composition of the tengerite-type structures has become clear.[21] Similarly, the use of high intensity synchrotron X-ray sources for examining much smaller crystals has become more routine in recent years. The gadolinium carbonate form of tengerite was synthesized hydrothermally and used as host lattice for Eu^{3+} activated phosphor powder.[6] Eu−Gd silicates were also synthesized hydrothermally and showed high emission quantum yields (up to 21.4%).[22] Layered rare earth hydroxides were very recently synthesized by the hydrothermal method.[23]

Here, we report two recently discovered gadolinium aquo carbonate structures containing ammonium or coordinated ammonia. The materials were prepared by hydrothermal synthesis with accompanying hydrolysis of urea. The carbonate resulting from the hydrothermal decomposition of urea is partially or completely anchored to the anionic layered $[Gd(CO_3)_2H_2O][NH_4]$ structure through strong covalent bonds to the metal. $[Gd_2(CO_3)_3NH_3H_2O]$ is a neutral 3-D covalent network containing embedded 2-D layers of the $[Gd(CO_3)_2H_2O][NH_4]$ structure but, bridged together by carbonate and the ammonium ion, is instead a coordinated ammonia ligand. Thermal characterization, vibrational spectroscopy, photoluminescence (PL), electron paramagnetic resonance (EPR), and room temperature magnetic susceptibility are reported for these new materials herein.

Experimental Section

Synthesis. $[Gd(CO_3)_2H_2O][NH_4]$ (which we denote SLUG-7, for University of California, Santa Cruz, Structure No. 7) was synthesized solvothermally under autogenous pressure. Solid $Gd(NO_3)_3 \cdot 6H_2O$ (99.9%, Acros) and urea (ACS reagent, Sigma-Aldrich) were added to deionized water in a 1:10:80 molar ratio, respectively. The total volume of the reaction mixture was scaled to 10 mL H_2O and added to a Teflon lined autoclave (constructed in-house). The 15 mL capacity autoclave was filled to about 2/3 capacity and heated statically in an oven at 150 °C for the layered structure $[Gd(CO_3)_2H_2O][NH_4]$ (SLUG-7) and at 175 °C for the 3-D structure $[Gd_2(CO_3)_3NH_3H_2O]$ (which we denote SLUG-8) for 48 h. The pH of the reactant solution increased from 4.8 to 9.4 during synthesis for SLUG-7 and to 9.7 for SLUG-8. The average yield was 86.4% (1.88 g) for SLUG-7 and 89.1% (1.75 g) for SLUG-8. Elemental anal. (Quantitative Technologies Inc., Whitehouse, NJ): 7.67% C (calcd 7.67%), 1.60% H (1.93%), and 4.69% N (4.47%) for SLUG-7 and 7.01% C (6.80%), 0.79% H (0.95%), and 2.60% N (2.65%) for SLUG-8.

Instrumental Details. Powder X-ray diffraction (PXRD) data were recorded using a Rigaku Americas MiniFlex Plus powder diffractometer (Cu Kα, $\lambda = 1.5418$ Å). Diffraction patterns were recorded from 2 to 40° 2θ, with a step size of 0.04° at a rate of 2° per minute. Single crystal data for SLUG-7 were recorded using a Bruker SMART APEX II CCD area detector X-ray diffractometer using graphite monochromated Mo Kα radiation ($\lambda = 0.71073$ Å). Crystallographic data for SLUG-8 were collected at Beamline 11.3.1 at the Advanced Light Source (ALS), Lawrence Berkeley National Laboratory ($\lambda = 0.77490$ Å). The structures were solved by direct methods and expanded routinely. The models were refined by full-matrix least-squares analysis of F^2 against all reflections. All non-hydrogen atoms were refined with anisotropic thermal displacement parameters. Thermal parameters for the hydrogen atoms were tied to the isotropic thermal parameter of the atom to which they are bonded. Programs used were as follows: APEX-II v2.1.4;[24] SHELXTL v6.14;[25] and Diamond v3.1e (demonstration version).[26]

Thermogravimetric analysis−mass spectrometry (TGA-MS) data were collected using a TA Instruments 2050 TGA with N_2(g) purge, coupled to a quadrupole sector mass spectrometer (Pfeiffer Vacuum Thermostar, GSD 301 T3) with 70 eV ionization potential. Samples were analyzed from ambient temperatures to 1000 °C at a rate of 10 °C per minute. Optical micrographs were obtained with an AxioCam MRc digital camera mounted on a Carl Zeiss Axioskop MAT optical microscope. PL measurements were performed using a Perkin-Elmer LS50-B photoluminescence spectrophotometer equipped with a solid-state sample holder. Samples were prepared by evaporating ethanol dispersions of finely ground microcrystals on glass slides. EPR spectra were measured on a Bruker EMX X-band spectrometer equipped with a constant flow cryostat. The field was 6000 gauss swept in 81.92 s with a time constant of 655 ms. The field was modulated at 100 kHz with an amplitude of 20 G. EPR spectra were recorded at a temperature of 123 K. Samples

(14) Yang, J.; Zhang, C. M.; Li, C. X.; Yu, Y. N.; Lin, J. *Inorg. Chem.* **2008**, *47* (16), 7262–7270.
(15) Hu, H.; Chen, Z. G.; Cao, T. Y.; Zhang, Q.; Yu, M. X.; Li, F. Y.; Yi, T.; Huang, C. H. *Nanotechnology* **2008**, *19*, 375702 (1–9).
(16) Yi, G. S.; Lu, H. C.; Zhao, S. Y.; Yue, G.; Yang, W. J.; Chen, D. P.; Guo, L. H. *Nano Lett.* **2004**, *4* (11), 2191–2196.
(17) Tamura, S.; Mori, A.; Imanaka, N. *Solid State Ionics* **2006**, *177* (26−32), 2727–2730.
(18) Hasegawa, I.; Tamura, S.; Imanaka, N. *Sens. Actuators, B* **2005**, *108* (1−2), 314–318.
(19) Mahalakshmi, M.; Arabindoo, B.; Palanichamy, M.; Murugesan, V. *J. Nanosci. Nanotechnol.* **2007**, *7* (9), 3277–3285.
(20) Wakita, H.; Nagashim, K. *Bull. Chem. Soc. Jpn.* **1972**, *45* (8), 2476–2479.
(21) Miyawaki, R.; Kuriyama, J.; Nakai, I. *Am. Mineral.* **1993**, *78* (3−4), 425–432.
(22) Ferdov, S.; Ferreira, R. A. S.; Lin, Z. *Chem. Mater.* **2006**, *18* (25), 5958–5964.
(23) Gandara, F. P. J.; Snejko, N.; Iglesias, M.; Gomez-Lor, B.; Gutierrez-Puebla, E.; Monge, M. A. *Angew. Chem., Int. Ed.* **2006**, *45* (47), 7998–8001.
(24) *APEX-II*, Version 2.1.4; Bruker-AXS: Madison, WI, 2007.
(25) *SHELXTL Crystal Structure Determination Package*; Bruker Analytical X-ray Systems Inc.: Madison, WI, 1995−99.
(26) Brandenburg, K.; Putz, H. *Diamond*, Version 3.1; Crystal-impact: Bonn, Germany, 2007.

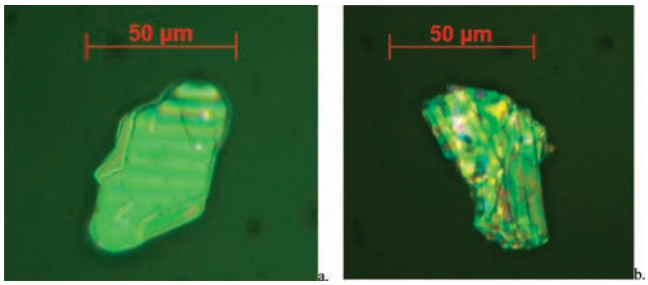

Figure 1. Optical micrographs (500× magnification) of crystals of SLUG-7 (a) and SLUG-8 (b).

were prepared by grinding 1 mg of sample per gram of KBr in an agate mortar and pestle and then placed in 4 mm OD quartz EPR tubes. Magnetic susceptibility was measured at room temperature using a Johnson Matthey magnetic susceptibility balance. Samples were prepared as fine powder in a 4 mm OD sample tube. Raman spectroscopy was carried out using a Renishaw micro-Raman setup using an Olympus optical microscope with 50× objective lens. The wavelength of the laser was 633 nm and was operated at 17.0 mW (Research Electro-Optics, Inc. Boulder, CO). Fourier transform infrared (FTIR) spectroscopy of the materials was accomplished using a Perkin-Elmer Spectrum One spectrophotometer. Samples were prepared as KBr disks.

Results and Discussion

SLUG-7 was synthesized with accompanying hydrothermal hydrolysis of urea and formed in high yield at a synthesis temperature of 150 °C. Below this optimal temperature for synthesis, no crystalline product forms. The thermal decomposition of urea has been used previously to prepare the gadolinium carbonate compounds $Gd_2(CO_3)_3 \cdot 2.5H_2O$ and $Gd_2O(CO_3)_2 \cdot H_2O$.[6] The carbonate anions formed by the hydrolysis of urea are chelated to gadolinium. In the case of SLUG-7, the ammonium also formed by the hydrolysis of urea appears in the final structure. The layers take on carbonate and a net negative charge, while the ammonium remains in the interlamellar space fulfilling charge neutrality.

The compound crystallizes in a colorless plate-like morphology (Figure 1a, Table 1), usually indicative of a layered crystalline material. The crystals exhibited a birefringence effect due to multilayer crystalline stacking and beveled crystals (Figure 1). Single crystals of suitable size were easily obtained for X-ray diffraction; the average size was about $60 \times 50 \times 20\ \mu m^3$ thin plates. The second compound, SLUG-8, is formed at a synthesis temperature of 175 °C. This structure has no overall charge on the framework. The crystals are again colorless plates (Figure 1b) but are made up of multicrystal stacks, which made selection of a suitable single crystal very challenging. The largest single crystal that could be obtained was $30 \times 30\ \mu m^2$ and less than 10 μm thick in the direction of stacking (Table 1).

Elemental analysis is consistent with the structural formulations obtained by single crystal X-ray diffraction (see Experimental Section). Both structures evolved gas upon exposure to hydrochloric acid, confirming the presence of carbonate in the structures. It is interesting to consider the interaction of carbonate formed by hydrolysis of urea, displacing nitrate from the starting gadolinium reagent. Carbon is only slightly less electronegative than nitrogen, giving oxygen increased electron density and therefore more strength to chelate gadolinium.

For the SLUG-7 structure, gadolinium is nine-coordinated by the oxygen atoms of four carbonate molecules and one water molecule (Figures 2a and 3a,b). The coordination geometry around gadolinium is that of a tricapped trigonal prism, commonly found in nine-coordinate compounds.[27,28] There are two types of carbonate molecules: the pendant carbonate which caps the layer and extends into the gallery space and the laterally bridging carbonates that define the layers. The carbonate that is extended into the interlamellar region is $\eta-2$ coordinating to a given gadolinium (Figure 3a,b and Table 2).

Each oxygen of the two intralayer carbonates is $\mu-2$ bridging with respect to gadolinium, connecting in the roughly [010] and [011] directions, resulting in extended two-dimensional layers. The bond angle between O(1) of the capping carbonate (nearly perpendicular to the layers in the *c* direction, Figure 3a), gadolinium, and O(4) is 80.24(14)°, while the O(1)−Gd−O(5) bond angle is 105.84(13)° (Figure 2a, Table 2). Thus, if these two bonds are bisected, the bridging carbonate molecule as a whole is nearly at a 90° angle from the Gd−O(1) bond. Both of the lateral carbonate molecules are symmetry equivalent (Figures 2a and 3a,b). The remaining two bonds to oxygen are from the $\mu-2$ intralayer bridging carbonates of the gadolinium on the other half of the double layer, as related by crystallographic mirror plane symmetry.

The two component layers within each SLUG-7 double layer are joined together by $\mu-2$ bridging oxygen atoms of the horizontally bridging carbonates, creating a corrugated layer (Figure 3b). Viewed down the *b*-axis, the double layer is partially held together by hydrogen bonding between the coordinated water molecules on each adjacent gadolinium atom and the pendant carbonate oxygens (Figure 3b). The layers are situated symmetrically as mirror images joined by bonds through the oxygen atoms when viewed in the $b-c$ plane (Figure 3a). The distance to the closest neighboring gadolinium atom is 4.1656(15) Å, beyond reasonable covalent bonding distance [median Gd−Gd contact distance ca. 3.693 Å by a search of the Cambridge Structural Database (CSD) and the Inorganic Crystal Structure Database (ICSD)].[29,30]

Ammonium ions also exist in the interlamellar space and are involved in an extensive hydrogen bonding network with the layers (Figure 3a,b and Table 3). The water molecules coordinated to gadolinium also form hydrogen bonds to the oxygen atoms of the capping

(27) Cotton, F. A.; Murillo, C. A.; Wilkinson, G.; Bochmann, M. *Advanced Inorganic Chemistry*, 6th ed.; John Wiley & Sons, Inc.: New York, 1999.
(28) Brewer, G.; Brewer, C.; Scheidt, W. R.; Shang, M. Y. *Inorg. Chem. Commun.* **2005**, *8* (8), 676–679.
(29) Allen, F. H. *Acta Crystallogr., Sect. B: Struct. Sci.* **2002**, *58*, 380–388.
(30) Hewat, P. *Inorganic Crystal Structure Database (ICSD)*; Fachinformationszentrum Karlsruhe (FIZ): Karlsruhe, Germany, 2007.

Table 1. Crystallographic Information, Data Collection, and Refinement Parameters for the Two Materials

structure	SLUG-7	SLUG-8
empirical formula	$GdH_6C_2NO_7$	$Gd_2H_5C_3NO_{10}$
formula weight ($g \cdot mol^{-1}$)	313.33	529.57
temperature (K)	150(2)	150(2)
wavelength (Å)	0.71073 (Mo Kα)	0.77490 (synchrotron)
crystal system	orthorhombic	monoclinic
space group	*Pbca*	*C*2
unit cell dimensions (Å)	$a = 6.051(3)$	$a = 15.287(2)$
	$b = 9.205(5)$	$b = 6.1941(9)$
	$c = 24.743(13)$	$c = 4.6631(7)$
		$\beta = 95.558(2)°$
volume ($Å^3$)	1378.2(12)	439.47(11)
Z	8	2
density (calculated, $g \cdot cm^{-3}$)	3.058	3.987
absorption coefficient (μ, mm^{-1})	9.637	15.009
F(000)	1168	472
crystal size (mm^3)	0.08 × 0.06 × 0.02	0.03 × 0.03 × 0.01
θ range for data collection (deg)	3.29 to 28.18	2.92 to 31.21
index ranges	$-8 \le h \le 8, -12 \le k \le 12, -32 \le l \le 32$	$-20 \le h \le 20, -8 \le k \le 8, -6 \le l \le 6$
reflections collected	12706	2805
independent reflections	1683 [$R_{int} = 0.0613$]	1093 [$R_{int} = 0.0287$]
completeness to θ	28.18° = 99.5%	31.21° = 100.0%
absorption correction	empirical	empirical
max and min transmission	0.8306 and 0.5133	0.3397 and 0.4335
refinement method	full-matrix least-squares on F^2	full-matrix least-squares on F^2
data/restraints/parameters	1683/0/118	1093/14/76
goodness of fit on F^2	1.033	1.173
final *R* indices [$I > 2\sigma(I)$]	$R_1 = 0.0265$, $wR_2 = 0.0495$	$R_1 = 0.0351$, $wR_2 = 0.0852$
R indices (all data)	$R_1 = 0.0440$, $wR_2 = 0.0548$	$R_1 = 0.0451$, $wR_2 = 0.0934$
largest diff. peak and hole	1.137 and −0.958 $e^- \cdot Å^{-3}$	4.855 and −1.527 $e^- \cdot Å^{-3}$

carbonate molecules that point into the interlayer space. All hydrogen atoms form strong hydrogen bonds to neighboring oxygen atoms.[31] The hydrogen bonding network bears resemblance to that of ice Ih,[32] which may be useful for intercalation of polar or gaseous molecules between the layers. The anionic charge on the layers could possibly be used as a host structure for cation intercalation/exchange. We are currently evaluating this structure for its propensity as a cation exchange material.

When the synthesis temperature is increased to 175 °C, the resultant structure is a more condensed, 3-D extended structure (SLUG-8) as evidenced by PXRD (Figure 4) and single crystal data (Figure 3c,d). In the case of this system, the higher synthesis temperature leads to a more condensed structure. A more compacted structure resulted where the intralayer ammonium ions have been driven out or coordinated to gadolinium as ammonia. The space between the layers (basal spacing) is 12.28 Å for SLUG-7, and in the case of SLUG-8, the majority basal (200) peak decreases to 7.57 Å (Figure 4). The small crystal size (30 × 30 × <10 μm, Figure 1, Table 1) of SLUG-8 made single crystal analysis extremely challenging. The SLUG-8 phase is essentially fine microcrystalline intergrown and stacked multicrystals. Data were successfully collected on the synchrotron beamline 11.3.1 at the Advanced Light Source at Lawrence Berkeley National Laboratory, through the SCrALS program (Service Crystallography at the Advanced Light Source).

The gadolinium is also nine-coordinate in SLUG-8 (Figure 3c,d and Table 4). The SLUG-8 phase is a condensed version of SLUG-7, where the double layers have been joined together by the pendant carbonates in the *c*-direction (*a*-direction in SLUG-8, Figure 3c,d). The connection of the layers causes a slight shift in the layer angle with respect to the cell edge, resulting in the $a-c$ angle being inclined and a monoclinic cell type. The intralayer ammonium cations that were present in SLUG-7 are absent although the coordinated water remains in the 3-D structure. Instead, the

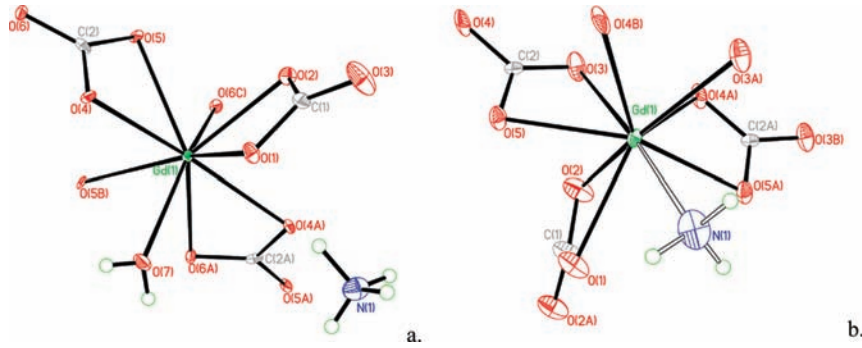

Figure 2. Oak Ridge thermal ellipsoid plot diagrams and atom labeling schemes of the coordination spheres of SLUG-7 (a) and SLUG-8 (b). Thermal ellipsoids are shown at 50% probability. The ammonia and water for SLUG-8 were found to be disordered at the same position; only the former is depicted here for clarity.

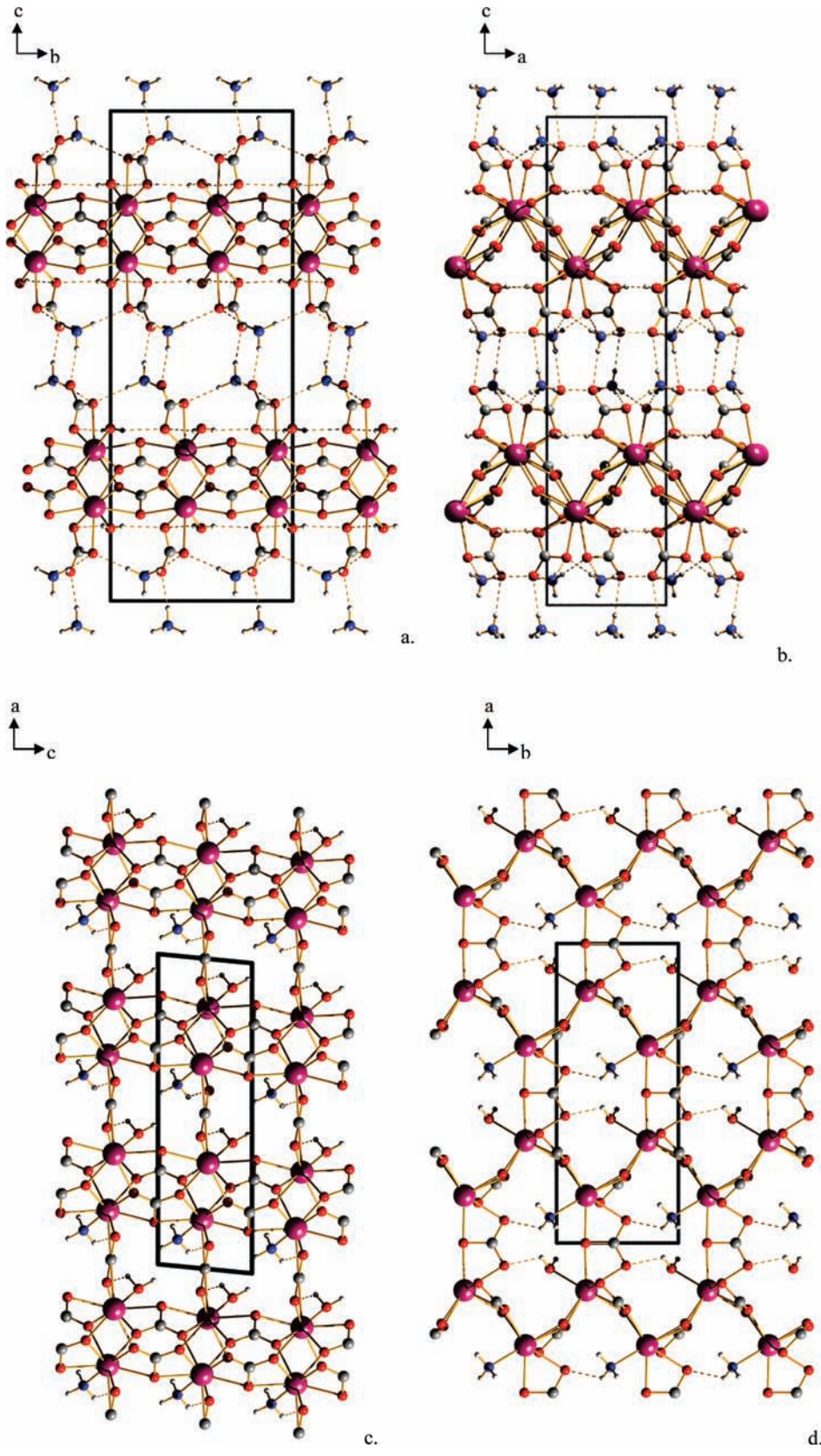

Figure 3. Crystallographic images of the two structures, with unit cell included (Gd = purple, C = gray, N = blue, O = red, H = light gray, and hydrogen bonds are represented as dashed yellow lines). View along the crystallographic *a*-axis of SLUG-7 shows the layers end-on (a). View in the *a*−*c* plane showing the corrugated layers (b). Images of SLUG-8 in the *a*−*c* plane (c) and the *a*−*b* plane (d).

ammonium appears to have been deprotonated and ammonia has ligated to gadolinium. The water and ammonia are included in the crystal structure as half-occupancy. Every other site contains water or ammonia.

Table 2. Bond Lengths (Å) and Angles (deg) in the Coordination Sphere of Gadolinium in SLUG-7[a]

Gd(1)−O(6)A	2.360(4)	Gd(1)−O(7)	2.386(5)
Gd(1)−O(1)	2.389(4)	Gd(1)−O(2)	2.417(4)
Gd(1)−O(4)	2.430(4)	Gd(1)−O(4)B	2.453(4)
Gd(1)−O(5)C	2.492(4)	Gd(1)−O(5)	2.499(4)
Gd(1)−O(6)B	2.508(4)		
O(7)−Gd(1)−O(1)	72.98(15)	O(1)−Gd(1)−O(2)	54.41(13)
O(7)−Gd(1)−O(2)	126.68(15)	O(7)−Gd(1)−O(4)	79.20(15)
O(1)−Gd(1)−O(4)	80.24(14)	O(2)−Gd(1)−O(4)	98.25(14)
O(7)−Gd(1)−O(5)	130.86(15)	O(1)−Gd(1)−O(5)	105.84(13)
O(2)−Gd(1)−O(5)	76.95(14)	O(4)−Gd(1)−O(5)	53.14(13)
O(6)A−Gd(1)−O(7)	150.91(15)	O(6)A−Gd(1)−O(4)	117.65(13)
O(6)A−Gd(1)−O(4)B	80.00(13)	O(1)−Gd(1)−O(4)B	82.54(14)
O(4)−Gd(1)−O(4)B	160.96(18)	O(7)−Gd(1)−O(5)C	79.27(15)
O(2)−Gd(1)−O(5)C	152.49(13)	O(4)B−Gd(1)−O(5)C	115.74(13)
O(4)B−Gd(1)−O(5)	141.07(13)	O(6)A−Gd(1)−O(6)B	79.26(9)
O(1)−Gd(1)−O(6)B	123.02(13)	O(4)−Gd(1)−O(6)B	133.78(13)
O(5)C−Gd(1)−O(6)B	63.57(12)	O(6)A−Gd(1)−O(1)	130.57(13)
O(6)A−Gd(1)−O(2)	76.78(14)	O(7)−Gd(1)−O(4)B	88.06(15)
O(2)−Gd(1)−O(4)B	78.01(13)	O(6)A−Gd(1)−O(5)C	82.21(13)
O(1)−Gd(1)−O(5)C	146.24(14)	O(4)−Gd(1)−O(5)C	75.96(13)
O(6)A−Gd(1)−O(5)	65.57(13)	O(5)C−Gd(1)−O(5)	78.29(9)
O(7)−Gd(1)−O(6)B	72.46(15)	O(2)−Gd(1)−O(6)B	127.95(13)
O(4)B−Gd(1)−O(6)B	52.59(12)	O(5)−Gd(1)−O(6)B	131.02(13)

[a] Symmetry transformations used to generate equivalent atoms. (A) $-x$, $y + 1/2$, $-z + 1/2$; (B) $-x + 1/2$, $y + 1/2$, z; (C) $x + 1/2$, y, $-z + 1/2$.

Table 3. Hydrogen Bonding Distances (Å) and Angles (deg) in SLUG-7[a]

D−H···A	d(D−H)	d(H···A)	d(D···A)	∠(DHA)
O(7)−H(7A)···O(2)G	0.74(7)	2.13(7)	2.845(6)	161(7)
O(7)−H(7B)···O(2)D	0.65(7)	2.15(7)	2.769(6)	159(9)
N(1)−H(1A)···O(1)	0.96(8)	1.94(8)	2.892(8)	171(6)
N(1)−H(1B)···O(3)G	0.77(8)	2.01(8)	2.769(8)	167(8)
N(1)−H(1D)···O(3)H	0.90(8)	1.88(8)	2.771(8)	169(7)

[a] Symmetry transformations used to generate equivalent atoms. (D) $-x + 1/2$, $y - 1/2$, z; (G) $x + 1$, y, z; (H) $x + 1/2$,$-y + 1/2$, $-z + 1$.

There is one hydrogen bond in the SLUG-8 structure; the proton distance on N(1)/O(6) to O(2) is 2.28 Å, and the donor−H−acceptor angle is 128.5° (Figure 3c,d). This bond is between the coordinated water or ammonia proton to the closest oxygen on the bridging carbonate. SLUG-8 is similar to the tengerite structure, though the rare earth carbonate tengerite-type structures all have an orthorhombic cell setting and contain no nitrogen.[20]

Thermal Characterization

TGA-MS traces of SLUG-7 indicate that the layered structure does not collapse to the more condensed structure upon heating to the synthesis temperature of SLUG-8 (Figure 5). Rather, ex situ heating and subsequent PXRD show that SLUG-7 decomposes into an amorphous powder mixture upon heating at or above 175 °C. The mass spectrum shows ammonium and water being evolved from the structure from the beginning of the measurement, possibly because of surface adsorption, and increasing in current near the onset of the majority of weight loss (18 *m/e*). Fragments were observed with the mass of 44 *m/e* and were attributed to CO_2^+. At 300 °C, about 10% of the original sample weight has been lost, corresponding to the loss of NH_4^+ ions and water molecules. The TGA trace slightly levels off at this point, coinciding with an increase in the 18 *m/e* mass spectrum (Figure 5). After the second major onset of mass loss around 625 °C, about 64% of the original mass remains,

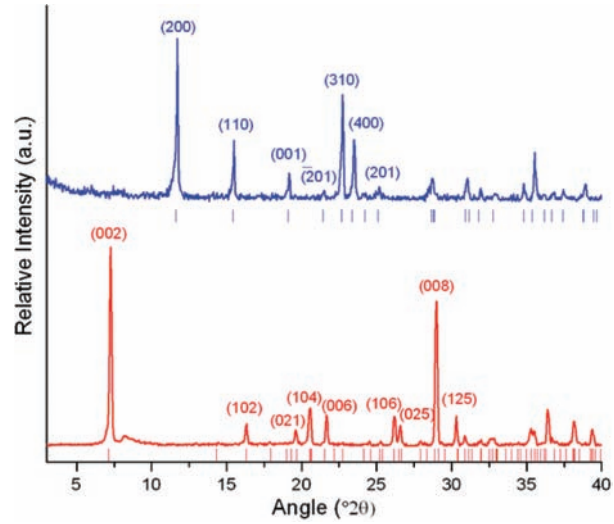

Figure 4. PXRD of SLUG-7 (bottom, red) and SLUG-8 (top, blue). Calculated theoretical powder diffraction patterns are shown beneath each pattern.

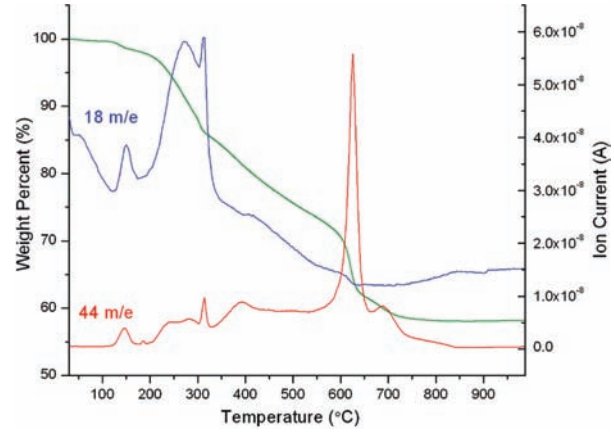

Figure 5. TGA-MS of SLUG-7 (TGA trace shown in green).

corresponding to only $Gd(CO_2)$ remaining (ca. 64.2%). By 900 °C, about 42% of the original sample weight has been lost, corresponding to the loss of ammonium, water, and 80% of the original carbonates.

TGA-MS shows relatively increased thermal stability for SLUG-8 up to about 325 °C (Figure 6), the calculated onset of weight loss. A slight decrease in the mass of about 2%, however, is observed from 30 °C up until the major onset of weight loss, likely because of physisorbed water. The mass spectrum shows the majority of mass loss is 18 *m/e* just above 350 °C, corresponding to loss of water. Ammonia is observed evolving from the structure as the 17 *m/e* fragment. The increase in the 44 *m/e* fragment signal at about 350 °C along with the water trace is due to CO_2^+. All three of the mass spectrum traces show a sharp increase at the major onset of weight loss at 325 °C. After the major mass loss, about 82% of the mass remains, corresponding to $Gd_2(CO_3)_2$ (ca. 82.1%). At 900 °C, about 68% of the original mass remains, corresponding to loss of ammonia, water, and 75% of the original carbonate molecules from the structure. All PXRD patterns after heating above 500 °C show amorphous powders.

Table 4. Bond lengths (Å) and Angles (deg) in the Coordination Sphere of Gadolinium in SLUG-8[a]

Gd(1)−O(1)	2.4388(8)	Gd(1)−O(4)A	2.400(11)
Gd(1)−O(2)	2.429(12)	Gd(1)−O(3)B	2.413(11)
Gd(1)−O(3)	2.538(11)	Gd(1)−O(5)C	2.444(10)
Gd(1)−O(5)	2.471(9)	Gd(1)−O(4)C	2.526(11)
Gd(1)−O(6)	2.432(14)		
O(2)−Gd(1)−O(3)	56.1(4)	O(2)−Gd(1)−O(6)	119.3(4)
O(2)−Gd(1)−O(1)	57.5(11)	O(2)−Gd(1)−O(5)	60.4(4)
O(1)−Gd(1)−O(3)	107.9(10)	O(4)A−Gd(1)−O(2)	132.1(4)
O(5)−Gd(1)−O(3)	52.3(3)	O(1)−Gd(1)−O(5)	73.0(4)
O(6)−Gd(1)−O(5)	125.4(4)	O(6)−Gd(1)−O(3)	175.3(4)
O(3)B−Gd(1)−O(5)C	77.5(4)	O(6)−Gd(1)−O(5)C	73.5(4)
O(4)A−Gd(1)−O(6)	100.2(4)	O(3)B−Gd(1)−O(1)	145.1(9)
O(4)A−Gd(1)−O(5)	75.3(3)	O(3)B−Gd(1)−O(3)	106.9(2)
O(5)C−Gd(1)−O(3)	106.0(3)	O(6)−Gd(1)−O(1)	67.5(10)
O(4)A−Gd(1)−O(4)C	108.3(2)	O(2)−Gd(1)−O(4)C	72.1(4)
O(1)−Gd(1)−O(4)C	121.2(10)	O(5)−Gd(1)−O(4)C	108.0(3)
O(4)C−Gd(1)−O(3)	56.7(3)	O(5)C−Gd(1)−O(4)C	52.9(3)
O(4)A−Gd(1)−O(3)B	60.0(4)	O(3)B−Gd(1)−O(2)	149.0(4)
O(3)B−Gd(1)−O(6)	77.6(4)	O(4)A−Gd(1)−O(1)	127.1(7)
O(4)A−Gd(1)−O(5)C	137.2(3)	O(2)−Gd(1)−O(5)C	82.9(4)
O(1)−Gd(1)−O(5)C	90.4(4)	O(3)B−Gd(1)−O(5)	133.5(4)
O(3)B−Gd(1)−O(4)C	76.9(4)	O(6)−Gd(1)−O(4)C	124.2(4)
O(5)C−Gd(1)−O(4)C	52.9(3)	O(4)A−Gd(1)−O(3)	83.3(4)

[a] Symmetry transformations used to generate equivalent atoms. (A) $-x + 3/2, y - 1/2, -z$; (B) $-x + 3/2, y - 1/2, -z + 1$; (C) $x, y, z + 1$.

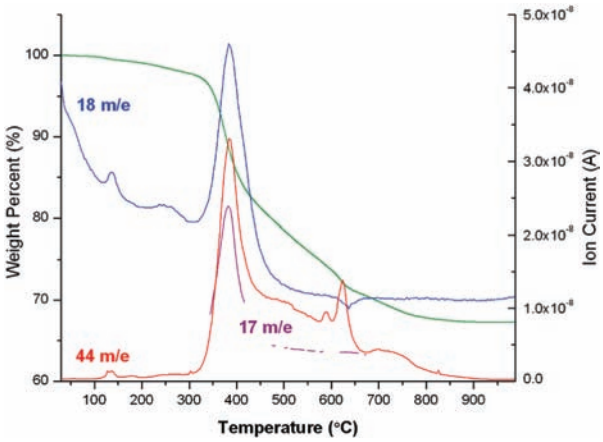

Figure 6. TGA-MS traces of SLUG-8 as the structure thermally decomposes.

The TGA-MS data initially suggest it may be possible to calcine the water and ammonia out of SLUG-8 at about 325 °C to render accessible channels. It was calculated, however, that there would only be about 30.4 Å^3 of void space if the water and ammonia molecules were removed, about the size of a water molecule (the program PLATON was used).[33] Upon ex situ heating beyond 600 °C and subsequent PXRD, the materials were again found to be amorphous powders.

Photoluminescence

Both materials show broad PL emission bands centered around 354 nm when excited at 250 nm in the solid state at ambient temperature, and this is due to a Gd(III) $^8S_{7/2} \leftarrow {}^6P_{7/2}$ transition (Figure 7).[34] Gadolinium(III) is known to exhibit a broad, long lasting phosphorescence under UV excitation at low temperatures and longer wavelengths.[35] There is a slight blue shift in the emission bands in SLUG-7 and SLUG-8 versus the starting material, which is a molecular salt. Aqueous $Gd(NO_3)_3 \cdot 6H_2O$ has one bidentate nitrate and another monodentate nitrate ligand coordinating gadolinium, while the third is solvated and not actually bound to the metal.[36] The blue shift may be a result of the increased rigidity of our carbonate extended structures. Emission spectra of both our materials show a shoulder at about 310 nm, just before the main emission peak at 354 nm. These bands may be from ligand-to-metal charge transfer transitions from the carbonate ligands.[37] The excitation spectra when excited at 365 nm in Figure 7 show two absorbance bands at 235 and 250 nm. When excited at 235 nm, the emission band intensity at 354 nm increases by about 31% as compared to excitation at 250 nm (not shown). The intensity of the PL increases in this order: starting material, 2-D structure, and 3-D structure. This trend seems to indicate a correlation between PL intensity and rigidity of the framework.

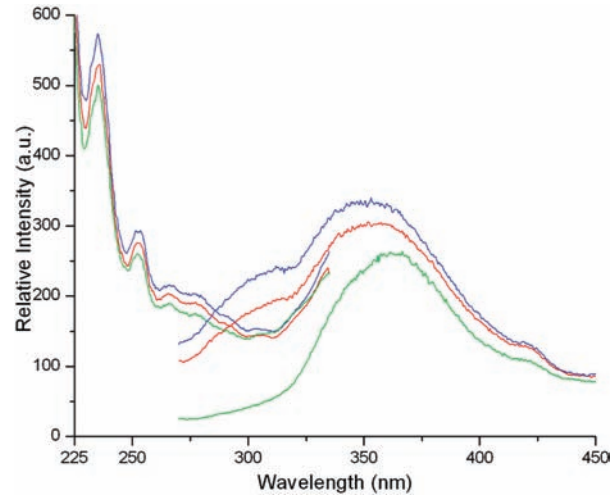

Figure 7. PL emission (270 to 450 nm; 250 nm excitation wavelength) and excitation spectra (225 to 340 nm; 365 nm excitation wavelength) of SLUG-7 (red), SLUG-8 (blue), and the $Gd(NO_3)_3$ starting reagent (green).

Vibrational Spectroscopy

Both materials show broad N−H stretching bands in the infrared region between 2800 and 3500 cm^{-1} because of ammonium in SLUG-7 and coordinated ammonia in SLUG-8 (Figure 8).[38] The infrared and Raman absorption band assignments are shown in Table 5. The infrared spectrum of SLUG-8 exhibits a sharp absorption at 3332 cm^{-1}, characteristic of coordinated ammonia.[38] For the starting $Gd(NO_3)_3 \cdot 6H_2O$ reagent, the O−H stretching absorption is

(31) Jeffrey, G. A. *An Introduction to Hydrogen Bonding*; Oxford University Press: New York, 1997.
(32) Goto, A.; Hondoh, T.; Mae, S. *J. Chem. Phys.* **1990**, *93*, 1412–1417.
(33) Spek, A. L. *J. Appl. Crystallogr.* **2003**, *36*, 7–13.
(34) Teotonio, E. E. S.; Brito, H. F.; Felinto, M. C. F. C.; Thompson, L. C.; Young, V. G.; Malta, O. L. *J. Mol. Struct.* **2005**, *751* (1−3), 85–94.
(35) Fernandes, J. A.; Ferreira, R. A. S.; Pillinger, M.; Carlos, L. D.; Jepsen, J.; Hazell, A.; Ribeiro-Claro, P.; Goncalves, I. S. *J. Lumin.* **2005**, *113* (1−2), 50–63.
(36) Nelson, D. I.; Irish, D. E. *J. Chem. Phys.* **1971**, *54* (10), 4479–4489.
(37) Zhou, Y. F.; Jiang, F. L.; Yuan, D. Q.; Wu, B. L.; Hong, M. C. *J. Mol. Struct.* **2005**, *743* (1−3), 21–27.
(38) Nakamoto, K. *Infrared and Raman Spectra of Inorganic and Coordination Compounds*, 5th ed.; John Wiley & Sons, Inc.: New York, 1997.

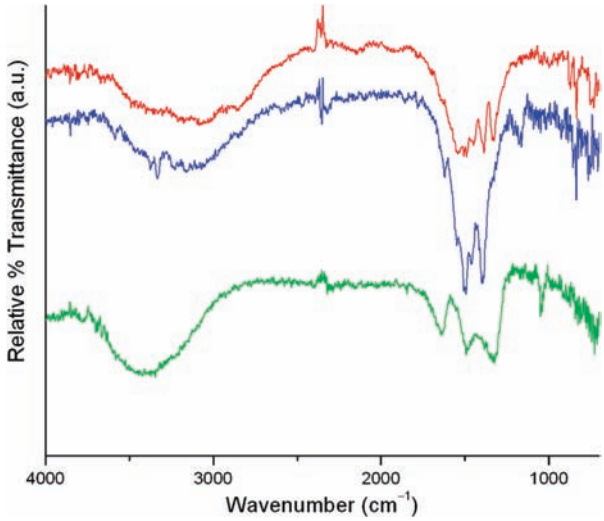

Figure 8. FTIR spectra of SLUG-7 (red), SLUG-8 (blue), and the starting material (green).

Table 5. Assignments of Raman and FTIR Vibrational Bands for Each Material

structure	vibrational mode[38−40]	Raman (cm^{-1})	infrared (cm^{-1})
SLUG-7	CO asymmetric stretch	1418	1493
	CO_2 symmetric stretch	1318	1327
	CO symmetric stretch	1054, 1093	1156
	coordinated H_2O rocking	774	750
	coordinated H_2O wagging	730	750
SLUG-8	CO asymmetric stretch	1437	1493
	CO_2 symmetric stretch	1398	1398
	CO symmetric stretch	1069, 1099	1163
	coordinated H_2O rocking	773	750
	coordinated H_2O wagging		750

observed in the 3000 to 3500 cm^{-1} range, presumably from the waters of hydration. SLUG-7 shows a lower frequency N−H stretch at 3217 cm^{-1}, presumably from the uncoordinated ammonium cations versus the coordinated ammonia. Another component of this band is present at about 2750 to 3000 cm^{-1}, also because of the ammonium ions. CO stretching was observed in the 1200 to 1700 cm^{-1} region for both structures from the various carbonate modes (Table 5). The rigidity of the structure increases from SLUG-7 to SLUG-8 as evidenced by the IR spectra. The CO stretching modes have shifted to higher energy as compared to the NO modes in the starting reagent, also increasing in intensity from SLUG-7 to SLUG-8.

The Raman spectra for both structures as well as the starting material are shown in Figure 9. Both new structures show strong vibrational transitions not present in the starting material; 1054 and 1093 cm^{-1} for SLUG-7 and 1069 and 1099 cm^{-1} for SLUG-8. These bands at higher wavenumber can be attributed to CO symmetric stretching from the bidentate carbonates chelating gadolinium (Table 5). There are water rocking and wagging modes observed at 730 and 774 cm^{-1} in SLUG-7 and at 773 cm^{-1} in SLUG-8 from the coordinated water molecules in both structures. In addition

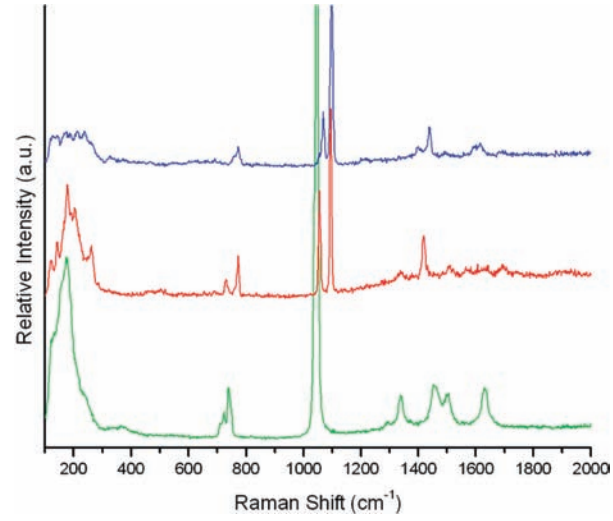

Figure 9. Raman spectra of starting reagent (green), SLUG-7 (red), and SLUG-8 (blue).

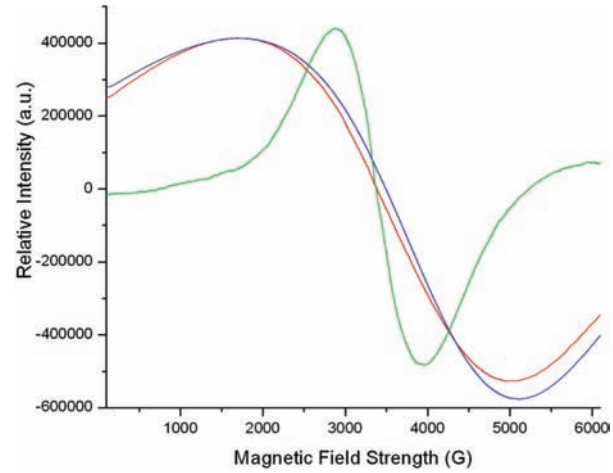

Figure 10. EPR spectra of the starting reagent (green), SLUG-7 (red), and SLUG-8 (blue).

to the H_2O wagging band at 730 cm^{-1} in SLUG-7, there is a vibrational absorption at 774 cm^{-1}, presumably because of the rocking mode of H_2O. In the Raman spectrum of SLUG-8, the H_2O wagging absorption is absent but another band appears at 773 cm^{-1} because of the H_2O rocking mode. Additional CO vibrational absorptions occur at 1418 and 1318 cm^{-1} for SLUG-7 and 1437 and 1398 cm^{-1} for SLUG-8. These modes are assigned to the CO asymmetric stretch and CO_2 symmetric stretch, respectively.

EPR Spectra

The EPR spectra of SLUG-7 and 8 (Figure 10) indicate there is spin communication between the gadolinium centers in these materials, manifested by the broadness of the transition because of dipolar broadening. The starting material $Gd(NO_3)_3 \cdot 6H_2O$ was also analyzed and showed a much sharper transition. The closest distance between neighboring gadolinium atoms in the starting salt is 7.521(5) Å, and none of the gadolinium atoms are bridged. In comparison, the nearest neighbors in SLUG-7 are 4.1655(15) Å and 4.1699(6) Å for SLUG-8, and both are bridged by oxygen atoms. No hyperfine splitting has been resolved for gadolinium isotopes

(39) Lin-Vien, D.; Colthup, N. B.; Fateley, W. G.; Grasselli, J. G. *The Handbook of Infrared and Raman Characteristic Frequencies of Organic Molecules*; Academic Press Inc.: San Diego, CA, 1991.
(40) Chen, L.; Shen, Y. H.; Xie, A. J.; Huang, F. Z.; Li, S. K.; Zhang, Q. F. *Cryst. Res. Technol.* **2008**, *43* (8), 797–800.

Table 6. Magnetic Parameters for the Two New Structures and the Starting Reagent

structure	SLUG-7	SLUG-8	$Gd(NO_3)_3 \cdot 6H_2O$
G	1.990	1.929	1.996
χ_m ($cm \cdot mol^{-1}$)	3.84×10^{-3}	5.55×10^{-3}	29.48×10^{-3}
μ_{eff} (μ_B)	3.02	3.63	8.36

or protons in general.[41] The G-values for the structures are listed in Table 6. Room temperature magnetic susceptibility measurements confirmed that these structures are paramagnetic (Table 6). The decreasing trend in effective magnetic moment (μ_{eff}) from the starting reagent to SLUG-7 indicates increasing spin correlation between neighboring gadolinium atoms in the extended structures. The experimental spin-only μ_{eff} of the starting reagent (8.36 μ_B) is close to the free ion spin-only magnetic moment of Gd^{3+} (7.94 μ_B) and is similar to that of other inorganic nitrate complexes of gadolinium at ambient temperatures (8.30 to 8.98 μ_B).[42,43]

Conclusions

These new lanthanide metal aquo carbonate structures are interesting from a standpoint of structural diversity. Prior to this report, there have been no layered framework gadolinium carbonate materials discovered.[29,30] The 2-D SLUG-7 structure, in which the layers are not "locked" together by carbonate, may be able to exchange its ammonium cations. The presence of isostructural layers in both the 2-D and the 3-D materials allow for an interesting comparison of both physical properties and mode of formation. These new structures represent significant progress toward the discovery of extended gadolinium based materials that may be useful in applications such as ion conduction, chemical sensing, gas storage, and magnetic materials. We are also exploring other rare earth analogues and mixed metal structures of these materials for increased PL activity from ions such as Er(III) and Eu(III).

Acknowledgment. This research was supported by an NSF Career Award (DMR-0506279). The single crystal X-ray diffraction data in this work were recorded on an instrument supported by the NSF Major Research Instrumentation (MRI) Program under Grant No. CHE-0521569. Samples for synchrotron crystallographic analysis were submitted through the SCrALS (Service Crystallography at Advanced Light Source) program. The ALS is supported by the U.S. Dept. of Energy, Office of Energy Sciences, under Contract DE-AC02-05CH11231. We thank Abraham Wolcott and Rebecca Newhouse of Professor Zhang's group in the department for assistance with photoluminescence and Raman spectroscopic measurements, respectively. We thank Dr. Eric Walter of Professor Millhauser's group for performing the EPR measurements.

Supporting Information Available: Crystallographic Information Files (CIF) containing refinement parameters, fractional atomic coordinates, and bond lengths and angles. This material is available free of charge via the Internet at http://pubs.acs.org.

IC801844B

(41) Sur, S. K.; Bryant, R. G. *J. Magn. Reson., Ser. B* **1996**, *111* (2), 105–108.
(42) Sherokalova, E. M.; Pleschov, V. G.; Baranov, N. V.; Korolev, A. V. *Phys. Lett. A* **2007**, *369* (3), 236–242.
(43) Stemmler, A. J.; Kampf, J. W.; Kirk, M. L.; Atasi, B. H.; Pecoraro, V. L. *Inorg. Chem.* **1999**, *38* (12), 2807–2817.